Chemical Bonding

DOI: 10.1002/anie.201409418

# Assessing the Viability of Extended Nonmetal Atom Chains in $M_nF_{4n+2}$ (M = S and Se)**

*Ivan A. Popov, Boris B. Averkiev, Alyona A. Starikova, Alexander I. Boldyrev,* Ruslan M. Minyaev,* and Vladimir I. Minkin**

***Abstract:*** *Theoretical investigations to evaluate the viability of extended nonmetal atom chains on the basis of molecular models with the general formula $M_nF_{4n+2}$ (M = S and Se) and corresponding solid-state systems exhibiting direct S–S or Se–Se bonding were performed. The proposed high-symmetry molecules were found to be minima on the potential energy surface for all $S_nF_{4n+2}$ systems studied (n = 2–9) and for selenium analogues up to n = 6. Phonon calculations of periodic structures confirmed the dynamic stability of the -$(SF_4–SF_4)_\infty$- chain, whereas the analogous -$(SeF_4–SeF_4)_\infty$- chain was found to have a number of imaginary phonon frequencies. Chemical bonding analysis of the dynamically stable -$(SF_4–SF_4)_\infty$- structure revealed a multicenter character of the S–S and S–F bonds. A novel definition and abbreviation (ENAC) are proposed by analogy with extended metal atom chain (EMAC) complexes.*

Cotton and co-workers introduced the chemical concept of extended metal atom chain (EMAC) complexes.[1] The first purple compound $[Ni_3(dpa)_4Cl_2]$ ($dpa^- =$ dipyridylamido anion) containing three Ni atoms was first reported in 1968.[2] However its correct structure was established only in 1991.[3] This structure contains a linear chain, Cl–Ni–Ni–Ni–Cl, surrounded by a spiral set of four dpa ligands. Since then similar compounds with three metal atoms, such as Cu, Co, Cr, and other transition metals, connected in a triatomic chain have been reported.[4] Tri-, tetra-, penta-, hepta-,[1,5] nona-,[6] deca-,[7] and hendecanuclear[8] EMACs surrounded by oligo-α-pyridylamino ligands have been synthesized and studied. In principle, it is thought that it would be possible to extend the system to an infinite one-dimensional molecule.[7] The trinuclear complex $[[Pt(Me_2Bpy)_2][PtCl_2(Me_2Bpy)]_2]^{2+}$ ($Me_2Bpy$ = 4,4′-dimethyl-2,2′-bipyridine) with Pt–Pt–Pt bonds has been shown to have relatively strong (about 40 kcal mol$^{-1}$) Pt–Pt metallic bonds with similar covalent and ionic contributions.[9] A huge number of other linear metal chains are known, such as $Li_2Sb$[10] with two linear Sb chains and $Au_2MP_2$ compounds (M = Hg, Pb, Tl) possessing Hg, Tl, and Pb chains.[11] As well as linear chains, different helical (Sb chains[12] in the crystal structure of KSb) and zigzag chains (P chains[11] in $Au_2MP_2$ (M = Hg, Pb, Tl) compounds; Sb chains[13] in the structure of $CaSb_2$; Ge chains[14] in the structure of $DyGe_3$) have also been reported. Progress made in the preparation and characterization of EMAC complexes has been reviewed.[15]

The number of molecules containing linear chains of nonmetal atoms is significantly smaller. Carbyne, an allotrope of carbon that forms large monoatomic linear chains with alternate single and triple carbon–carbon bonds, has a long history in chemistry.[16] Boron, by acquiring an extra electron, forms unbranched linear monoatomic chains of boron atoms surrounded by lithium cations.[17] Linear phosphorus–boron chains[18] and double-helical lithium–phosphorous[19] chains have been studied theoretically. It was reported that there are two phases with helical structures made up of triangular and squared chains of sulfur that are stable at 1.5 GPa and temperatures from 300 to 1100 K.[20] Interestingly, selenium can also form the helical squared chain structures in a similar way to sulfur.[20] Analogous oxygen helical structures are also found under the pressure of metallization.[21,22] The crystal structures of $TeF_4$, $SeF_4$,[23] and more recently $SF_4$[24] have been reported. Notably, in all these tetrafluorides, there is no direct M–M bonding (M = Te, Se, S).

Herein we present the computational results for $M_nF_{4n+2}$ molecules (M = S, Se) with a monoatomic chain structure based on direct S–S or Se–Se bonding. We refer to these species as extended nonmetal atom chain (ENAC) compounds by analogy with extended metal atom chain (EMAC) complexes.

According to our calculations, the staggered structure I with $D_{4d}$ symmetry is a true minimum on the potential energy surface (PES), in agreement with the experimental data[25] (Figure 1). We performed the search (ca. 2500 trial structures) for the global minimum and low-lying isomers of $S_2F_{10}$ by the Coalescence Kick method[26] and found out that there were no other unfragmented isomers that were more stable than isomer I. In fact, the most stable isomer existed as two distinct

[*] I. A. Popov, Prof. Dr. A. I. Boldyrev
Department of Chemistry and Biochemistry, Utah State University
Logan, UT 84322 (USA)
E-mail: a.i.boldyrev@usu.edu
B. B. Averkiev
ISP/Applied Sciences Laboratory, Washington State University
Spokane, WA 99210-1495 (USA)
A. A. Starikova, Prof. Dr. R. M. Minyaev, Prof. Dr. V. I. Minkin
Institute of Physical and Organic Chemistry
Southern Federal University
194/2 Stachka Ave., Rostov-on-Don 344090 (Russian Federation)
E-mail: minyaev@ipoc.sfedu.ru
minkin@ipoc.sfedu.ru

[**] This research was supported by the National Science Foundation (CHE-1361413). R.M.M. thanks the Russian Ministry of Education and Science for financial support within the State Assignment for Research (Project Part, project N4.71.2014/K). Computer, storage and other resources from the Division of Research Computing in the Office of Research and Graduate Studies at Utah State University are gratefully acknowledged.

Supporting information for this article is available on the WWW under http://dx.doi.org/10.1002/anie.201409418.

  

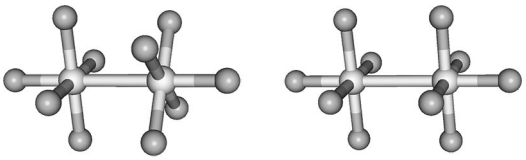


***Figure 1.*** Molecular structures of the staggered (I) and eclipsed (TS1) structures of $S_2F_{10}$ at 0 K and their relative energies (in kcal mol$^{-1}$) at M06-2X/6-311+G(2df) and CCSD(T)/cc-pVTZ//M06-2X/6-311+G(2df) (shown in square brackets), both corrected for zero-point energies at the DFT level.

parts: octahedral $SF_6$ and $SF_4$ with a seesaw shape. Interestingly, two other close-lying isomers, which were also fragmented, were found to be very high in energy (see Figure S1 in the Supporting Information). The eclipsed structure TS1 with $D_{4h}$ symmetry is a first-order saddle point on the PES and corresponds to a barrier of 9.6 kcal mol$^{-1}$ (DFT) or 9.1 kcal mol$^{-1}$ (CCSD(T)) for rotation about the S–S σ bond.

The experimentally determined distance $R$(S–S) = 2.274(5) Å in $S_2F_{10}$ is appreciably longer than the corresponding distance in $S_2H_2$: $R$(S–S) = 2.055 Å,[27] which suggests the presence of a single S–S σ bond. Since the S–S distance is quite dependent on the electronegativity of X in $S_2X_2$ species (X = H, Li, Na, F, Cl, Br, I), as was recently shown by El-Hamdi et al.,[28] the S–S distance in $S_2F_{10}$ was also compared with that in $S_2F_2$. Experimental data show a slightly decreased value ($R$(S–S) = 1.888 Å),[29] although the bond order is expected to be the same as in $S_2H_2$. The values for the S–S bond-dissociation energy (BDE) of $S_2F_{10}$, $S_2H_2$, and $S_2F_2$ were found to be 41.8, 66.6, and 77.3 kcal mol$^{-1}$, respectively, thus confirming the bond weakening in $S_2F_{10}$, which is partly due to F···F repulsion and sulfur–fluorine electron transfer.[30]

Chemical bonding analysis of $S_2F_{10}$ performed by natural bond orbital (NBO)[31,32] and adaptive natural density partitioning (AdNDP)[33] methods (see Figure S2c) revealed that the S–$F_{eq}$ and S–$F_{ax}$ bonds are classical with occupation number (ON) values close to the ideal value of 2.00 | e |, whereas the S–S σ bond has a rather low ON value of 1.45 | e | (NBO) or 1.58 | e | (AdNDP). According to NBO analysis, every 2c–2e S–F bond is formed by $3s3p^33d^2$ hybrid atomic orbitals (AOs) of sulfur and primarily 2p AOs of fluorine with a small contribution of 2s AOs. Since those bonds are highly polarized towards fluorine (only about 20% of the electron density comes from sulfur), the resulting occupation of 3d AOs is rather small. NBO analysis also revealed that valence non-Lewis density is 2.08 | e | (2.53% of the valence electron density), which is a sign of some multicenter contribution to the bonding. Since the NBO method requires and maintains strict local (and global) orthogonality between all NBOs, the only way to make five S–F bonds and one S–S bond whose S hybrids are orthogonal and pointed towards the vertices of an octahedron is by placing d-character in the hybrids. Thus, the d-character appears as a result of orthogonalization. The occupation of 3d orbitals can be evaluated from the composition of 10 S–F bonds and one S–S bond. According to our calculations, the occupation of the 3d AOs of S is 0.90 | e |. This value is substantially higher than the corresponding value found by natural electron configuration (NEC) analysis, which is completely independent from the natural population analysis in the bonding description. NEC analysis for the $S_2F_{10}$ molecule shows the following occupation on the S atom: $3s^{1.14}3p^{2.30}4s^{0.01}3d^{0.18}$, which proves little involvement of d orbitals in the active valence space. In general, this kind of problem can occur when a delocalized system is forced to be described by a single localized configuration. Therefore, we believe that both S–S and S–F bonds should be described by the multicenter bonding. AdNDP analysis allowed us to search for the 3c–4e bonding on the $F_{eq}$–S–$F_{eq}$ fragments. Indeed, we found that eight equatorial fluorine atoms can be described by 3c–4e bonds with an ON value of 2.00 | e | (see Figure S2d). Within the AdNDP method we could also search for a 12-centered 2-electron (12c–2e) σ bond instead of the 2c–2e S–S σ bond. This user-directed approach showed that the ON of the 12c–2e σ bond is 2.00 | e | with about 0.4 | e | distributed among equatorial fluorine atoms with antibonding character (see Figure S2d). This result is consistent with S–S σ-bond elongation and weakening in $S_2F_{10}$ relative to $S_2H_2$ and $S_2F_2$ (see Figure S2 for comparative illustrations of chemical bonding in $S_2H_2$, $S_2F_2$, and $S_2F_{10}$).

Our calculations showed that $S_2F_{10}$ is not thermodynamically stable towards dissociation into $SF_6 + SF_4$ by 23.3 kcal mol$^{-1}$ at the DFT level and by 27.7 kcal mol$^{-1}$ at CCSD(T)/cc-pVTZ//M06-2X/6-311+G(2df). These numbers provide us with some insight on the expected errors for larger systems. These results are in agreement with the experimental observation[34] that $S_2F_{10}$ decomposes slowly in an inert container above 150 °C into $SF_6 + SF_4$ (see Figure S3). By following the dissociation path, we found the $SF_6$–$SF_4$ transition state TS2 (see Figure S4). The barrier for the $S_2F_{10} \rightarrow SF_6 + SF_4$ process is 66.4 kcal mol$^{-1}$ at the DFT level and corresponds to TS2. Thus, this thermodynamically unstable molecule is very stable kinetically. We found that all $S_nF_{4n+2}$ molecules studied ($n$ = 2–9; see Figure S5) in $D_{4d}$ (even $n$) and $D_{4h}$ (odd $n$) conformations are minima on the PES, although all of them are thermodynamically unstable towards the $S_{n-1}F_{4(n-1)+2} + SF_4$ dissociation channel (see Table S1 in the Supporting Information).

We also searched for possible alternative structures of the proposed chainlike structures along the series $S_nF_{4n+2}$ ($n$ = 2–9), in which direct S–S bonding is expected, but failed to find any structures lower in energy that corresponded to a minimum on the PES. Calculation of the periodic boundary conditions (PBCs) for the -$(SF_4–SF_4)_\infty$- system resulted in the following geometrical parameters: $R$(S–S) = 2.36 Å and $R$(S–F) = 1.62 Å (CASTEP); $R$(S–S) = 2.38 Å and $R$(S–F) = 1.63 Å (VASP). Both bonds are slightly longer than those in molecular species: the S–S bond was found to be longer than that in $S_2F_{10}$ (2.274 Å), and the S–F bonds appear to be longer than the mean S–F bond length in $S_2F_{10}$ (1.569 Å) and in $SF_6$ (1.5623 Å).[35]

We also performed PBC calculations for the molecular crystal of $SF_4$, which has the space group $P2_12_12_1$ according to experimental data.[24] It turned out that the molecular crystal of $SF_4$ is more stable than our -$(SF_4–SF_4)_\infty$- system by

  

21.7 kcal mol$^{-1}$ per $SF_4$ group. This result is consistent with our calculations for the molecular species (see Table S1), for which the dissociation energy for the $S_nF_{4n+2} \rightarrow S_{n-1}F_{4(n-1)+2} + SF_4$ channel was found to be approximately 22 kcal mol$^{-1}$. A plot of phonon dispersions in the Brillouin zone (see Figure S6) showed that no imaginary phonon frequency is observed in the whole Brillouin zone, thus indicating the dynamic stability of the -$(SF_4–SF_4)_\infty$- linear chain.

For chemical bonding analysis of the periodic system, we utilized a newly developed solid-state AdNDP (SSAdNDP) algorithm[36] in conjunction with general and user-directed searches (see the Supporting Information for details). The resulting picture is shown in Figure 2b. Similar to the results derived for the $S_2F_{10}$ molecule, the use of SSAdNDP enabled direct classical S–F and S–S σ bonds to be found with ON values of 1.96 and 1.61 |e|, respectively. However, according to NEC analysis, the S atom has the following occupation of orbitals: $3s^{1.44}3p^{2.48}4s^{0.01}3d^{0.17}$, which is very similar to that of $S_2F_{10}$. Therefore, we believe that the initially found eight 2c–2e S–F bonds should be described as four 3c–4e bonds in the $F_{eq}$–S–$F_{eq}$ fragments shown in Figure 2b as a combination of bonding and nonbonding orbitals. User-directed SSAdNDP analysis enabled a 10c–2e bond (with eight fluorine atoms included within one unit cell) to be found instead of a 2c–2e S–S σ bond. This approach gave us an ON(10c–2e bond) value of 1.98 |e|, which shows that approximately 0.4 |e| is distributed among fluorine atoms with antibonding character, similar to the situation in $S_2F_{10}$. Importantly, the AdNDP results derived for the molecular $S_nF_{4n+2}$ systems ($n = 2$–9) are also in agreement with the SSAdNDP calculations.

Although we are not aware of any experimental data on the $Se_2F_{10}$ molecule, our calculations show that the staggered $D_{4d}$ structure I is a true minimum on the PES. The eclipsed TS3 structure corresponds to a torsional barrier of 4.7 kcal mol$^{-1}$ at the DFT level (see Figure S7).

The Se–Se BDE of $Se_2F_{10}$ was found to be 27.9 kcal mol$^{-1}$, whereas the Se–Se BDE values of $Se_2H_2$ and $Se_2F_2$, in which a single Se–Se σ bond is expected, are 51.0 and 60.1 kcal mol$^{-1}$, respectively, thus also confirming the bond weakening in $Se_2F_{10}$. These values are supported by the corresponding bond lengths: $R$(Se–Se) = 2.47 Å in $Se_2F_{10}$, $R$(Se–Se) = 2.33 Å in $Se_2H_2$, $R$(Se–Se) = 2.20 Å in $Se_2F_2$.

Initial AdNDP and NBO analyses of $Se_2F_{10}$ show that Se–$F_{eq}$ and Se–$F_{ax}$ σ bonds are classical with ON(Se–$F_{eq}$) = 1.95–2.00 |e| and ON(Se–$F_{ax}$) = 2.00 |e|, whereas the Se–Se σ bond has a rather low ON value of 1.33 |e| (NBO) or 1.51 |e| (AdNDP). Similar to the $S_2F_{10}$ molecule, we believe that the chemical bonding in $Se_2F_{10}$ should be described by multicenter bonding: 3c–4e bonding on the $F_{eq}$–Se–$F_{eq}$ fragments and a 12c–2e bond instead of a 2c–2e Se–Se σ bond. Again, the low ON of the Se–Se σ bond in $Se_2F_{10}$ is in concordance with its elongation and weakening relative to those in $Se_2H_2$ and $Se_2F_2$.

We also found that the $Se_2F_{10}$ molecule is not thermodynamically stable by 31.4 kcal mol$^{-1}$ at the DFT level and dissociates into $SeF_6 + SeF_4$ (see Figure S8). The barrier for the $Se_2F_{10} \rightarrow SeF_6 + SeF_4$ process is 45.6 kcal mol$^{-1}$ at the DFT level and corresponds to TS4 (see Figure S9). Similar to the $S_2F_{10}$ molecule, thermodynamically unstable $Se_2F_{10}$ is very stable kinetically.

Geometry optimizations of the $Se_nF_{4n+2}$ molecules revealed that high-symmetry molecules containing a linear chain of Se atoms are minima on the PES up to $n = 6$. At $n = 7$, the high-symmetry structures are no longer minima, since the $F_4$ fragments are slightly shifted relative to each other, thus resulting in lower symmetry ($C_4$, $D_4$ geometries; see Figure S10). In spite of this irregularity, the Se–Se σ-bond lengths remain almost the same upon chain elongation (see Table S2). It was found that all the $Se_nF_{4n+2}$ molecules studied were thermodynamically unstable

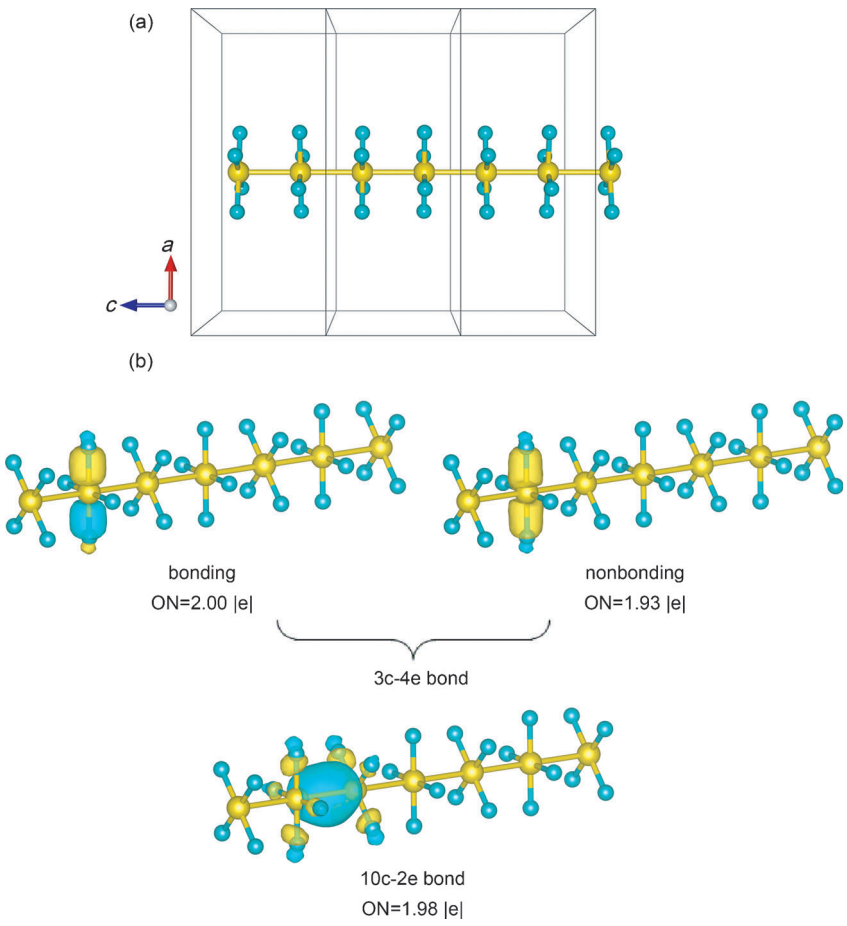


***Figure 2.*** a) Structure of the infinite -$(SF_4–SF_4)_\infty$- system with the corresponding unit cells. b) Representative bonds identified by SSAdNDP analysis: one 10c–2e bond, one 3c–4e $F_{eq}$–S–$F_{eq}$ bond. A total of 24 lone pairs (1c–2e bonds) on eight fluorine atoms within one unit cell with ON = 1.94-1.98 |e| are omitted for clarity. Direct coordinates of the $S_2F_8$ unit cell used for the SSAdNDP analysis are given in Table S3 of the Supporting Information.

towards the $Se_{n-1}F_{4(n-1)+2} + SeF_4$ dissociation channel with about the same energy value of around 30 kcal mol$^{-1}$ (see Table S2).

The proposed infinitely long one-dimensional -($SeF_4$–$SeF_4$)$_\infty$- system was found to possess the following geometrical parameters: $R$(Se–Se) = 2.58 Å and $R$(Se–F) = 1.76 Å (CASTEP), and $R$(Se–Se) = 2.64 Å and $R$(Se–F) = 1.78 Å (VASP). Direct coordinates of its unit cell are given in Table S4. Although the proposed high-symmetry $Se_nF_{4n+2}$ molecules ($n$ = 2–6) were shown to be local minima on the PES, the phonon-density-of-states calculations revealed a number of imaginary phonon frequencies for -($SeF_4$–$SeF_4$)$_\infty$-, thus showing its dynamic instability. Despite its instability, we performed SSAdNDP analysis on -($SeF_4$–$SeF_4$)$_\infty$- for comparison with the results obtained for its sulfurous analogue (see the Supporting Information).

In conclusion, we have computationally assessed the viability of $M_nF_{4n+2}$ molecules (M = S, Se; $n$ = 2–9) as well as infinitely long chains based on direct S–S or Se–Se bonding and surrounded by fluorine atoms. We found that these molecules are not thermodynamically stable with respect to the $M_nF_{4n+2} \rightarrow M_{n-1}F_{4(n-1)+2} + MF_4$ dissociation channel. However, high energy barriers for the $M_2F_{10} \rightarrow MF_6 + MF_4$ processes cause us to believe that these ENAC compounds are also viable species. We propose a novel definition and, consequently, a novel abbreviation (ENAC) by analogy with EMAC complexes. PBC calculations confirm the dynamic stability of the -($SF_4$–$SF_4$)$_\infty$- chain. For this chain, no imaginary phonon frequency was observed in the whole Brillouin zone, whereas the analogous -($SeF_4$–$SeF_4$)$_\infty$- chain was found to have plenty of imaginary phonon frequencies. We hope that our results will inspire experimentalists to synthesize these interesting one-dimensional chemical species.

Received: September 24, 2014
Revised: November 7, 2014
Published online: December 4, 2014

**Keywords:** chemical bonding · computational chemistry · electronic structure · nonmetal atom chains · sulfur/selenium compounds

[1] J. F. Berry in *Multiple Bonds between Metal Atoms* (Eds.: F. A. Cotton, C. A. Murillo, R. A. Walton), Springer, New York, **2005**, pp. 669 – 706.
[2] T. J. Hurley, M. A. Robinson, *Inorg. Chem.* **1968**, *7*, 33 – 38.
[3] S. Aduldecha, B. J. Hathaway, *J. Chem. Soc. Dalton Trans.* **1991**, 993 – 998.
[4] R. Clérac, F. A. Cotton, L. M. Daniels, K. R. Dunbar, C. A. Murillo, I. Pascual, *Inorg. Chem.* **2000**, *39*, 752 – 756.
[5] J. F. Berry in *Struct. Bond.*, *Vol. 136* (Ed.: G. Parkin), Springer, Berlin, **2010**, pp. 1 – 28.
[6] S.-M. Peng, C.-C. Wang, Y.-L. Jang, Y.-H. Chen, F.-Y. Li, C.-Y. Mou, M.-K. Leung, *J. Magn. Magn. Mater.* **2000**, *209*, 80 – 83.
[7] J.-H. Kuo, T.-B. Tsao, G.-H. Lee, H.-W. Lee, C.-Y. Yeh, S.-M. Peng, *Eur. J. Inorg. Chem.* **2011**, 2025 – 2028.
[8] R. H. Ismayilov, W.-Z. Wang, G.-H. Lee, C.-Y. Yeh, S.-A. Hua, Y. Song, M.-M. Rohmer, M. Bénard, S.-M. Peng, *Angew. Chem. Int. Ed.* **2011**, *50*, 2045 – 2048; *Angew. Chem.* **2011**, *123*, 2093 – 2096.
[9] A. Poater, S. Moradell, E. Pinilla, J. Poater, M. Solà, M. A. MartÍnez, A. Llobet, *Dalton Trans.* **2006**, 1188 – 1196.
[10] a) W. Müller, *Z. Naturforsch.* **1977**, *32*, 357 – 359; b) G. A. Papoian, R. Hoffmann, *Angew. Chem. Int. Ed.* **2000**, *39*, 2408 – 2448; *Angew. Chem.* **2000**, *112*, 2500 – 2544.
[11] M. Eschen, W. Jeitschko, *J. Solid State Chem.* **2002**, *165*, 238 – 246.
[12] K. Seifert-Lorenz, J. Hafner, *Phys. Rev. B* **1999**, *59*, 843 – 854.
[13] a) K. Deller, B. Eisenmann, *Z. Anorg. Allg. Chem.* **1976**, *425*, 104; b) K. Deller, B. Eisenmann, *Z. Naturforsch.* **1976**, *31*, 1146.
[14] K. Albert, H.-J. Meyer, R. Hoffmann, *J. Solid State Chem.* **1993**, *106*, 201 – 210.
[15] a) *Extended Linear Chain Compounds*, *Vols. 1 – 3* (Ed.: J. S. Miller), Plenum, New York, **1982**; b) R. Hoffmann, *Solids and Surfaces*: *A Chemist's View of Bonding in Extended Structures*, VCH, New York, **1988**; c) J. K. Bera, K. R. Dunbar, *Angew. Chem. Int. Ed.* **2002**, *41*, 4453 – 4457; *Angew. Chem.* **2002**, *114*, 4633 – 4637.
[16] M. Liu, V. I. Artyukhov, H. Lee, F. Xu, B. I. Yakobson, *ACS Nano* **2013**, *7*, 10075 – 10082.
[17] M. Wörle, R. Nesper, *Angew. Chem. Int. Ed.* **2000**, *39*, 2349 – 2353; *Angew. Chem.* **2000**, *112*, 2439 – 2443.
[18] D. Jacquemin, M. Medved, E. A. Perpète, *Int. J. Quantum Chem.* **2005**, *103*, 226 – 234.
[19] A. S. Ivanov, A. J. Morris, K. V. Bozhenko, C. J. Pickard, A. I. Boldyrev, *Angew. Chem. Int. Ed.* **2012**, *51*, 8330 – 8333; *Angew. Chem.* **2012**, *124*, 8455 – 8458.
[20] O. Degtyareva, E. Gregoryanz, M. Somayazulu, P. Dera, H. K. Mao, R. J. Hemley, *Nat. Mater.* **2005**, *4*, 152 – 155.
[21] Z. Wang, Y. Wang, G. Zou, H. K. Mao, Y. Ma, *Proc. Natl. Acad. Sci. USA* **2012**, *109*, 751 – 753.
[22] J. Sun, M. Martinez-Canales, D. D. Klug, C. J. Pickard, R. J. Needs, *Phys. Rev. Lett.* **2012**, *108*, 045503.
[23] R. Kniep, L. Korte, R. Kryschi, W. Poll, *Angew. Chem. Int. Ed. Engl.* **1984**, *23*, 388 – 389; *Angew. Chem.* **1984**, *96*, 351 – 352.
[24] J. T. Goettel, N. Kostiuk, M. Gerken, *Angew. Chem. Int. Ed.* **2013**, *52*, 8037 – 8040; *Angew. Chem.* **2013**, *125*, 8195 – 8198.
[25] a) R. B. Harvey, S. H. Bauer, *J. Am. Chem. Soc.* **1953**, *75*, 2840 – 2846; b) H. Oberhammer, O. Lösking, H. Willner, *J. Mol. Struct.* **1989**, *192*, 171 – 175.
[26] A. P. Sergeeva, B. B. Averkiev, H. J. Zhai, A. I. Boldyrev, L. S. Wang, *J. Chem. Phys.* **2011**, *134*, 224304.
[27] E. Herbst, G. Winnewisser, *Chem. Phys. Lett.* **1989**, *155*, 572 – 575.
[28] M. El-Hamdi, J. Poater, F. M. Bickelhaupt, M. Solà, *Inorg. Chem.* **2013**, *52*, 2458 – 2465.
[29] R. L. Kuczkowski, *J. Am. Chem. Soc.* **1964**, *86*, 3617 – 3621.
[30] I. Novak, *Inorg. Chim. Acta* **1991**, *181*, 81 – 83.
[31] A. E. Reed, L. A. Curtiss, F. Weinhold, *Chem. Rev.* **1988**, *88*, 899 – 926.
[32] a) J. P. Foster, F. Weinhold, *J. Am. Chem. Soc.* **1980**, *102*, 7211 – 7218; b) F. Weinhold, C. R. Landis, *Valency and Bonding*, *A Natural Bond Orbital Donor – Acceptor Perspective*, Cambridge University Press, Cambridge, **2005**.
[33] D. Y. Zubarev, A. I. Boldyrev, *Phys. Chem. Chem. Phys.* **2008**, *10*, 5207 – 5217.
[34] W. R. Trost, R. L. McIntosh, *Can. J. Chem.* **1951**, *29*, 508 – 525.
[35] H. M. Kelley, M. Fink, *J. Chem. Phys.* **1982**, *77*, 1813 – 1817.
[36] T. R. Galeev, B. D. Dunnington, J. R. Schmidt, A. I. Boldyrev, *Phys. Chem. Chem. Phys.* **2013**, *15*, 5022 – 5029.
[37] a) A. D. Becke, *J. Chem. Phys.* **1993**, *98*, 5648 – 5652; b) C. Lee, W. Yang, R. G. Parr, *Phys. Rev. B* **1988**, *37*, 785 – 789.
[38] J. P. Perdew, K. Burke, M. Ernzerhof, *Phys. Rev. Lett.* **1996**, *77*, 3865 – 3868.
[39] Y. Zhao, D. G. Truhlar, *Theor. Chem. Acc.* **2008**, *120*, 215 – 241.
[40] M. S. Gordon, J. S. Binkley, J. A. Pople, W. J. Pietro, W. J. Hehre, *J. Am. Chem. Soc.* **1982**, *104*, 2797 – 2803.

  

[41] a) T. H. Dunning, *J. Chem. Phys.* **1989**, *90*, 1007 – 1023; b) N. B. Balabanov, K. A. Peterson, *J. Chem. Phys.* **2005**, *123*, 064107.
[42] Gaussian 09 (Revision B.0.1), M. J. Frisch, et al., Gaussian, Inc., Wallingford CT, **2009**.
[43] G. Kresse, J. Furthmüller, *Comput. Mater. Sci.* **1996**, *6*, 15 – 50.
[44] P. E. Blöchl, *Phys. Rev. B: Condens. Matter Mater. Phys.* **1994**, *50*, 17953 – 17979.
[45] G. Kresse, D. Joubert, *Phys. Rev. B: Condens. Matter Mater. Phys.* **1999**, *59*, 1758 – 1775.
[46] S. J. Clark, M. D. Segall, C. J. Pickard, P. J. Hasnip, M. I. J. Probert, K. Refson, M. C. Payne, *Z. Kristallogr.* **2005**, *220*, 567 – 570.
[47] H. J. Monkhorst, J. D. Pack, *Phys. Rev. B* **1976**, *13*, 5188 – 5192.
[48] K. Refson, P. R. Tulip, S. J. Clark, *Phys. Rev. B* **2006**, *73*, 155114.
[49] a) I. A. Popov, A. I. Boldyrev, *Comput. Theor. Chem.* **2013**, *1004*, 5 – 11; b) I. A. Popov, V. F. Popov, K. V. Bozhenko, I. Černusàk, A. I. Boldyrev, *J. Chem. Phys.* **2013**, *139*, 114307; c) I. A. Popov, W.-L. Li, Z. A. Piazza, A. I. Boldyrev, L.-S. Wang, *J. Phys. Chem. A* **2014**, *118*, 8098 – 8105.
[50] I. A. Popov, Y. Li, Z. Chen, A. I. Boldyrev, *Phys. Chem. Chem. Phys.* **2013**, *15*, 6842 – 6848.
[51] B. D. Dunnington, J. R. Schmidt, *J. Chem. Theory Comput.* **2012**, *8*, 1902 – 1911.
[52] K. Momma, F. Izumi, *J. Appl. Crystallogr.* **2011**, *44*, 1272 – 1276.
[53] U. Varetto, *Molekel 5.4.0.8*, Swiss National Supercomputing Centre, Manno (Switzerland).

  